SLAC-PUB-6036
January 1993
(T/E)

Measurement of Higgs Boson Branching Fractions*

Michael D. Hildreth

Stanford Linear Accelerator Center
Stanford University, Stanford, CA 94309

ABSTRACT

We describe methods one can employ at a $\sqrt{s}$ = 500 GeV e^+e^- linear collider to measure the branching fractions of a Higgs boson. These methods select one Higgs decay mode above all others with high purity, leaving measureable Standard Model backgrounds as the only source of contamination. Integrated luminosities of 50fb^{-1} are required to obtain statistical errors of 10-20% on the branching fractions to $b\bar{b}$, $\tau^+\tau^-$, and $WW^{(*)}$. For an intermediate mass Higgs this is sufficient to distinguish the MSSM from the Standard Model Higgs over most of the Supersymmetric parameter space.

I. Introduction

The nature of Electroweak Symmetry Breaking remains as one of the last unexplored frontiers in our understanding of the Electroweak interactions. The standard $SU(2)_L \times U(1)$ model of these interactions [1] predicts a neutral scalar (H) called the Higgs particle which breaks the symmetry of the Electroweak interaction and gives mass to the fundamental fermions. Supersymmetric models [2], such as the Minimal Supersymmetric extention to the Standard Model (MSSM), predict a cadre of Higgs particles for the same purpose. Testing these models to truly understand the nature of the Higgs particle will be a crucial experiment if such a particle is discovered at a future colliding-beam facility such as SSC/LHC, NLC, or LEP-II. Since the different models of Higgs interactions systematically differ in the way the Higgs couples to the known standard model

*Work supported by Department of Energy contract DE-AC03-76SF00515

Invited talk presented at the Workshop on Electroweak Symmetry Breaking at Colliding-Beam Facilities, Santa Cruz, CA, December11-12, 1992

particles, measuring these couplings is a natural and sensitive way to distinguish between the competing theories. Thus, measurements of the branching fractions of the Higgs boson are sensitive probes into the nature of the Higgs couplings. It is generally agreed that a linear collider [3] would be the most powerful experimental setting for establishing a detailed picture of the Higgs boson, since one could use the full power of techniques developed for physics at these machines, such as beam-energy constraints, and kinematic fits, among others. Here, after a brief introduction to general parameters of a $\sqrt{s}$ = 500 GeV e^+e^- linear collider, we present general techniques for measuring the branching fraction of an intermediate-mass Higgs to as many of the standard model particles as possible.

II. Introduction to the NLC

The next generation e^+e^- linear collider (NLC) is envisioned as an expandable machine, with an initial center of mass energy $\sqrt{s}$ = 300-500 GeV. Since the energy is not fixed, this machine will be able to explore any physics at energies below the full machine energy, including the toponium threshold. The upgrade to center of mass energies of 1-1.5 TeV would proceed at a later date. A possible layout for a proposed NLC is shown in Figure 1. The trombone-like arms of the pre-acceleratror and main linac can easily be extended if neccessary to allow an increase in the energy.

The design luminosities for these machines have to be quite large in order to compensate for the $1/s$ behaviour of the non-resonant point cross-sections. Table 1 lists several different proposed NLC designs and their typical luminosity parameters. Typically, for a year of running, integrated luminosities of 50 fb^{-1} or so can be expected, where a canonical year is defined as 10^7 seconds. One important accelerator design parameter that has the potential to adversely effect the ability of the experimenters to do useful physics is the spectrum of the initial state radiation from the colliding beams. Tightly focussed bunches of electrons and positrons will radiate in the magnetic field of the on-coming bunch

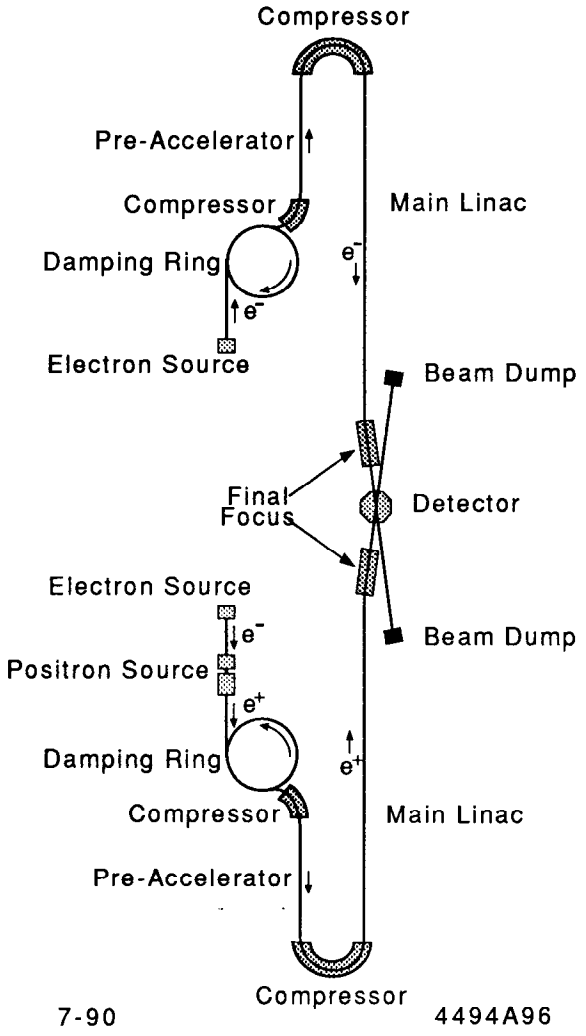

Figure 1. A proposed layout of the NLC

	Design Luminosity (cm^{-2} s^{-1})	
	500 GeV	1 TeV
SuperC (Tesla) :	5×10^{33}	1×10^{34}
S-Band (DESY) :	4×10^{33}	0.3×10^{34}
X-Band (NLC/JLC) :	6×10^{33}	2×10^{34}

Table 1. Design parameters for several linear colliders

as they pass through each other. (See figure 2.) This process is called "beamstrahlung" and is controlled by the severity of the deflection introduced by the beam-beam interaction, which is directly related to the final beam size at the interaction point.

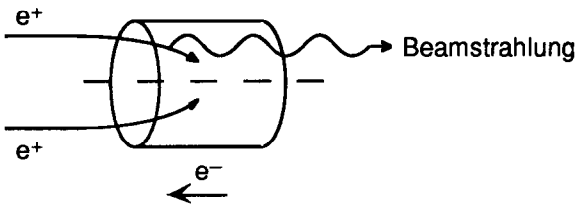

Figure 2. Beamstrahlung

Figure 3 shows four different center of mass energy spectra, three from beamstrahlung with varying degrees of disruption, and the fourth from initial state radiation alone. As can be seen, the mild

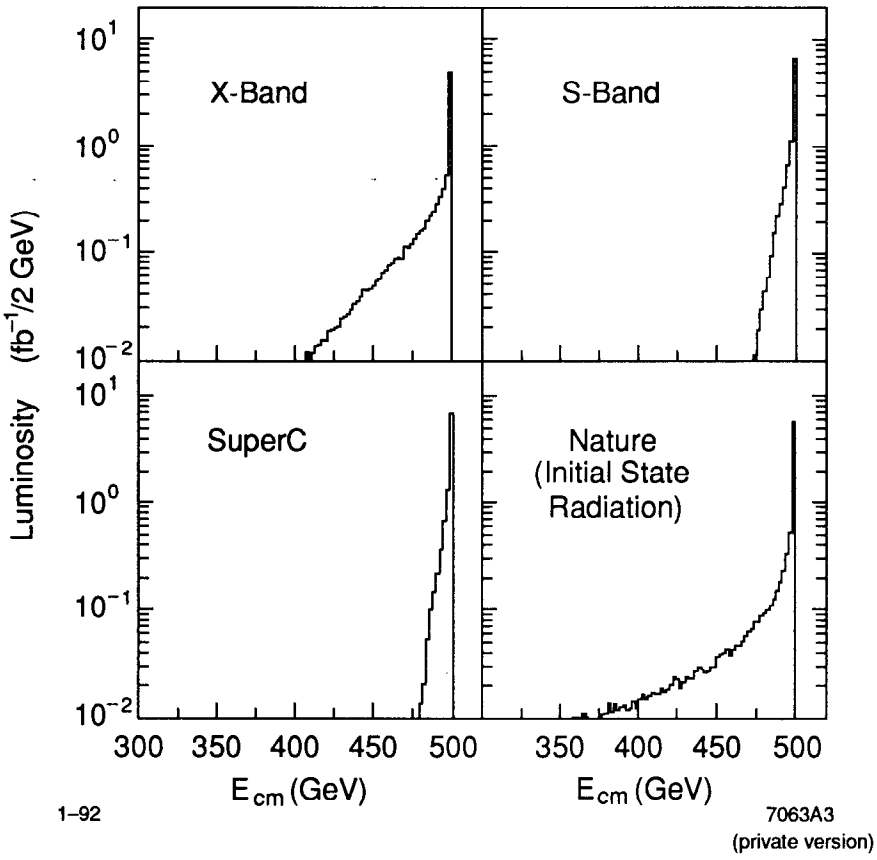

Figure 3. Center of mass energy spectra for several linear collider designs compared to initial state radiation.

cases are much less severe than the initial state radiation present in nature itself. It can also be shown [4] that the radiation is almost always due to only one of the initial state particles, not both. This allows one to do kinematic fits where the missing momentum along the beam axis and the missing energy are the same.

At these energies, the dominant cross-sections are due to electroweak and QCD processes. Figure 4 shows a plot of the cross section for the processes $e^+e^- \rightarrow W^+W^-$ and $e^+e^- \rightarrow q\bar{q}$. At 500 GeV, one unit of R corresponds to 4000 events per year at typical design luminosities. For integrated luminosities of 50 fb^{-1} at center of mass energies around 500 GeV, these background processes contribute more than one million events per year to the data volume. It should be emphasized that these standard model processes (and others with much lower cross-sections, such as $e^+e^- \rightarrow ZZ$ and $e^+e^- \rightarrow WWZ$) are the *only* significant sources of backgrounds for most physics analyses, including studies of the Higgs.

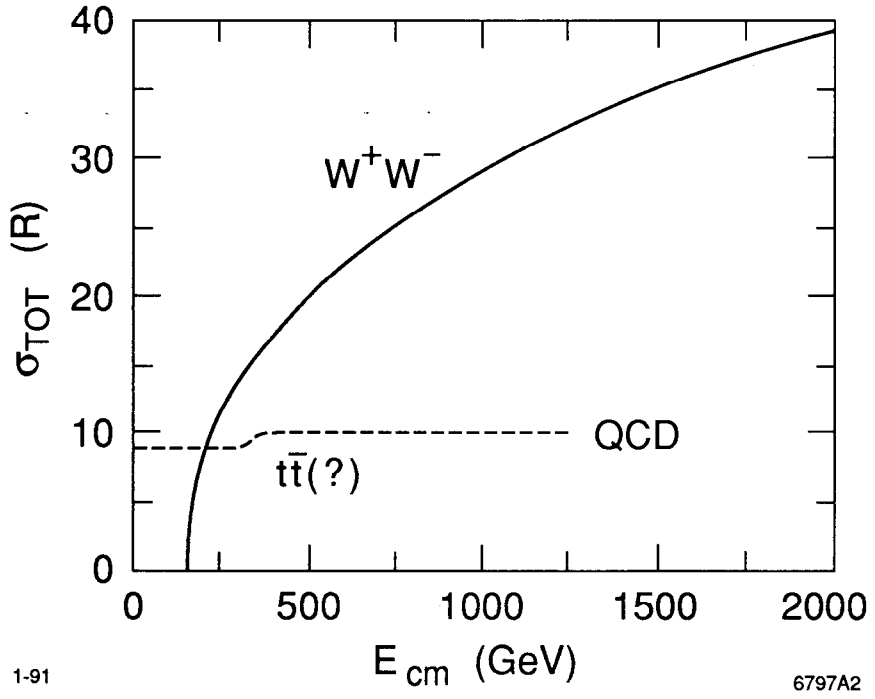

Figure 4. Production cross-sections for the dominant Standard Model processes at high energy.

III. Measurement of Higgs Branching Fractions

If a Higgs boson is discovered at a future accelerator, it will be imperative to learn as much as possible about the Higgs so as to understand the true nature of electroweak symmetry breaking. Besides its mass, the parameters which determine the relationship of the Higgs to the standard model are its couplings to the standard model particles. This presents the experimenter with a series of measureable constants:

- *Vector Boson Couplings*

These can be determined by measuring the total cross-section for the Bjorken bremsstrahlung process $e^+e^-\rightarrow ZH$, or by measuring the branching fractions for $H\rightarrow WW^{(*)}$ and $H\rightarrow ZZ^{(*)}$ if the mass of the Higgs is large enough.

- *Higgs-fermion Couplings*

These can be determined for light fermions by measuring the branching fractions for $H\rightarrow b\bar{b}$, $H\rightarrow c\bar{c}$, and $H\rightarrow \tau^+\tau^-$. The coupling between the Higgs and the top can be derived from measuring the total cross-section for ttH bremsstrahlung, or by measuring the branching fraction for $H\rightarrow gg$.

As can be seen from the above list, measurements of the Higgs branching fractions will be sensitive probes into the nature of the Higgs. To illustrate the potential of this method, Figure 5(a) shows the branching fractions of the standard model Higgs boson as a function of its mass, while Figure 5(b) gives the branching fractions of the lightest *CP*-even Higgs in the MSSM as a function of the ratio of the supersymmetric vacuum expectation values $\tan\beta$ [5], where the Higgs mass is chosen to be 120 GeV. Note the difference in the branching fraction to boson pairs for the two cases, especially to W pairs. The branching fraction for this mode is non-negligible even down to Higgs masses of 110 GeV, making it potentially the most useful in distiguishing the Standard Model Higgs from the MSSM Higgs over a large range in $\tan\beta$.

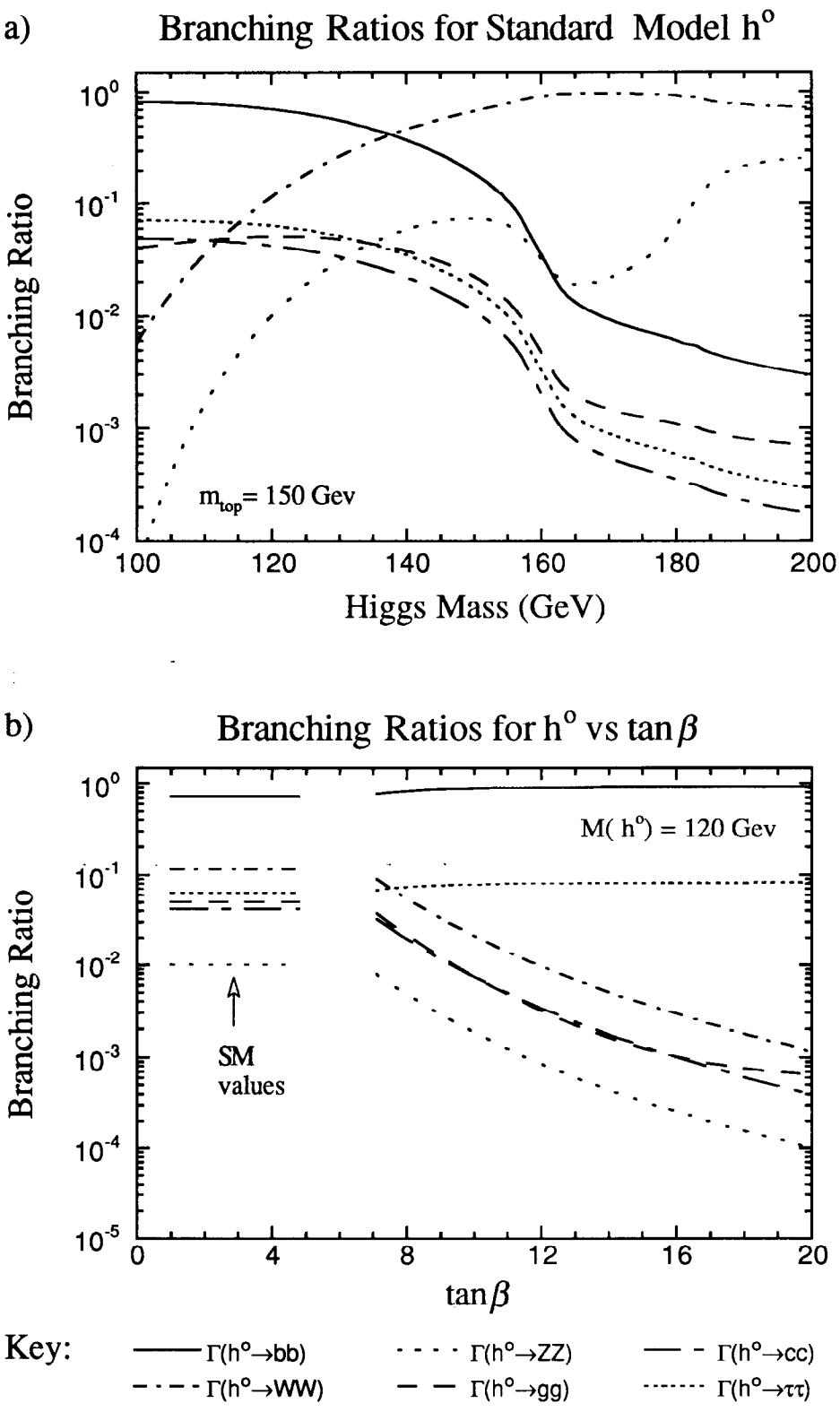

Figure 5. (a) Branching fractions of the Standard Model Higgs boson as a function of its mass for a 150 GeV top quark mass. **(b)** Branching fractions of the lightest *CP*-even Higgs in the MSSM as a function of tanβ, for a top quark mass of 175 GeV. An explanation of plot symbols is given below the plot.

A. General Analysis Techniques

Before entering into a detailed description of the branching fraction measurement, we present an exposition of several techniques that will be used throughout the following analyses.

• *B (or anti-B) tag*

A high-precision vertex detector is used to distinguish those tracks which miss the event origin by an amount significantly larger than the error on the measured distance. These analyses assume that the impact parameter b, the three-dimensional distance-of-closest approach to the interaction point, can be measured with the following precision:

$$\sigma(x\text{-}y)_b \cong \sqrt{5\mu\text{m}^2 + \left[\frac{50\mu\text{m}}{p\sqrt{\sin^3\theta}}\right]^2}$$

in the transverse direction, and

$$\sigma(z)_b \cong \sqrt{20\mu\text{m}^2 + \left[\frac{50\mu\text{m}}{p\sqrt{\sin^3\theta}}\right]^2}$$

along the beam axis. These resolutions are comparable to those obtained by the SLD collaboration with a CCD pixel vertex detector [6].

One identifies events containing b quarks by counting the number of tracks having large values of $b_{\text{norm}} = b/\sigma_b$. Table 2 shows that this method can be used to distinguish and accept $H\rightarrow WW^{(*)}$ events while rejecting $H\rightarrow b\bar{b}$ events with high efficiency. This can be seen graphically in Figure 6, which shows the distributions of the number of high impact parameter tracks with significance greater than 3 per event for several different Higgs decay modes. Note that, as would be expected, the distribution for $H\rightarrow b\bar{b}$ has a rather long tail due to the long lifetime of the b quark. Since the tracks from $H\rightarrow WW^{(*)}$ and $H\rightarrow gg$ come predominantly from light quarks, these distributions peak at zero tracks, while the distribution for $H\rightarrow c\bar{c}$ peaks somewhere between. This may prove to be a useful tool in

distinguishing $H \rightarrow c\bar{c}$ events from the other events containing light quarks, and hence measuring the branching fraction for $H \rightarrow c\bar{c}$.

# tracks with $b_{norm}>3$	efficiency for $H \rightarrow WW^{(*)}$	efficiency for $H \rightarrow b\bar{b}$
0	0.334	0.006
1	0.594	0.016
2	0.769	0.043
3	0.889	0.104
4	0.944	0.184
5	0.976	0.296
6	0.990	0.432
7	0.995	0.563

Table 2. Efficiencies for event tags based on counting tracks with large impact parameters with a precision vertex detector.

• *Beam-Constrained Fits*

Given our prior knowledge of the center-of-mass energy and the fact that initial-state radiation is likely to be from only one of the initial state fermions, one can perform kinematic fits of different types to reconstruct the four-vectors of the underlying partons in the event. An example case which will be used later is shown in Figure 7, an $H \rightarrow WW^{(*)}$ event in which one of the Ws has decayed via $W \rightarrow l\nu$, and there is an initial-state radiation photon present.

We can apply the following energy and momentum constraints to this event:

- $E_{vis} = 2\ E_{beam}$
- $\Sigma p_x = \Sigma p_y = 0$
- $\Sigma p_z = p_{ISR}$

to fit for the missing momentum carried away by the neutrino.

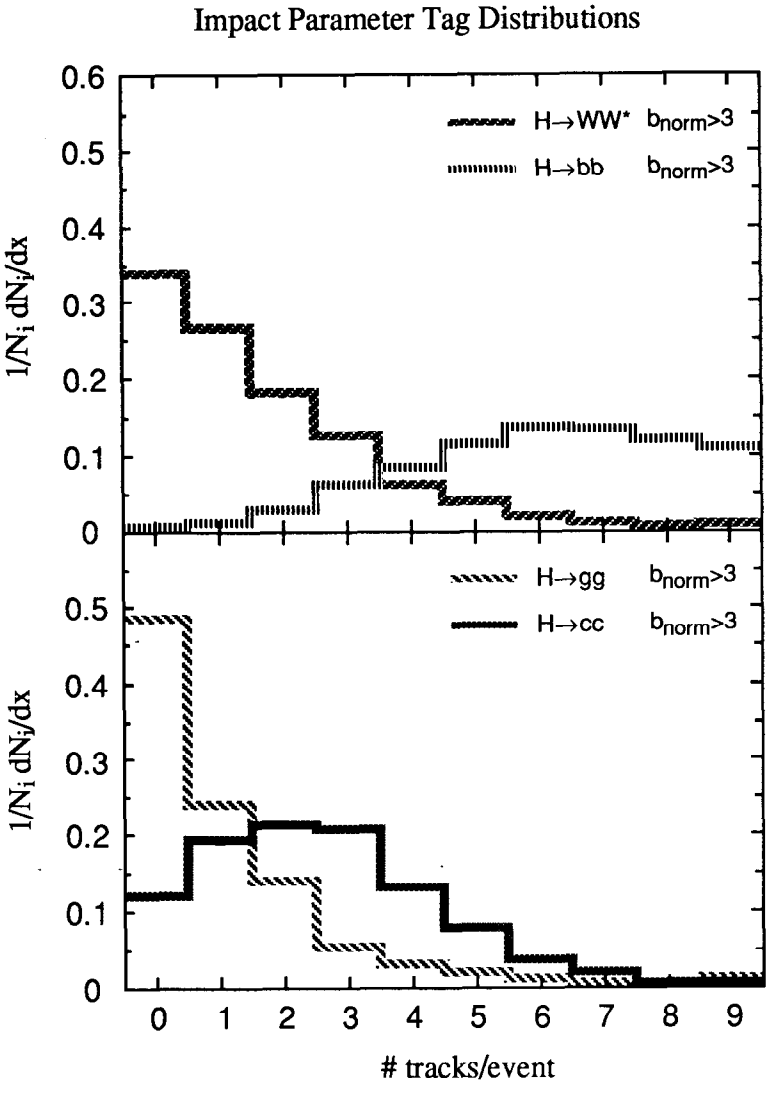

Figure 6. The distributions of number of tracks with impact paramter significance greater than 3 for several Higgs decay modes. The plots show purely the expected shapes of the distributions; no assumptions on branching fractions have been made.

Since we assume that the Higgs mass is known we can add additional constraints, such as

- M_{Higgs} = Reconstructed Mass
- $E_Z = \gamma_{obs}\, m_Z$

to make the fit more accurate. This specific fit will be used later in the study of the branching fraction for $H \rightarrow WW^{(*)}$.

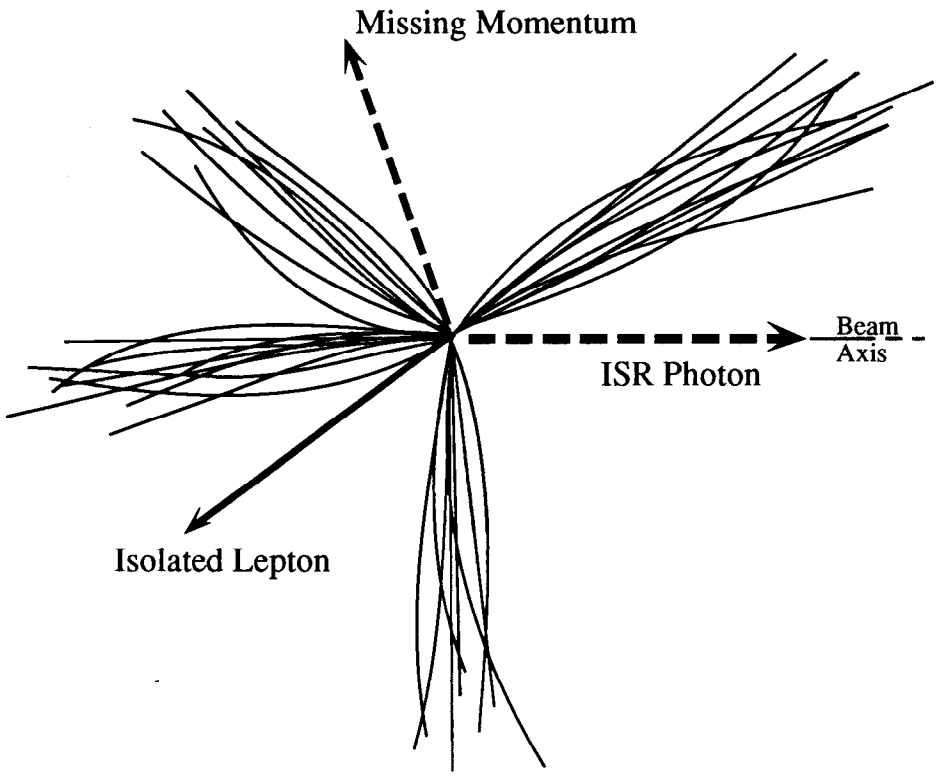

Figure 7. An $H \rightarrow WW^{(*)}$ event in which one of the Ws has decayed via $W \rightarrow l\nu$, and there is an initial-state radiation (ISR) photon present.

B. Simulation Description

Since many of the analyses presented here depend on knowing the initial beam energy and total momentum of the event, we have chosen to consider only Higgs events produced by the Bjorken process (Figure 8).

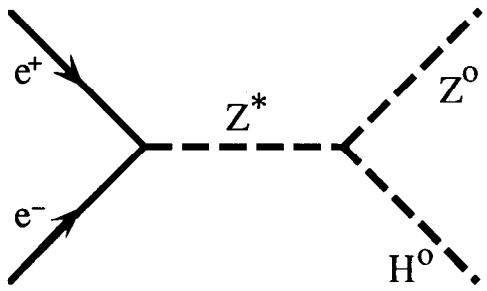

Figure 8. The Bjorken production mechanism for the Higgs.

This approach is only practical for lighter Higgs masses, as the cross-section for this process falls off dramatically as the Higgs mass becomes large. In this study, the center-of-mass energy is 400 GeV, and the candidate Higgs mass is 140 GeV, which falls into the range where all of the Higgs decays into Standard Model particles have (potentially) measurable rates. (See Figure 5.) Background processes included in this study are $e^+e^- \rightarrow W^+W^-$, $e^+e^- \rightarrow ZZ$, $e^+e^- \rightarrow q\bar{q}$, $e^+e^- \rightarrow t\bar{t}$, and $e^+e^- \rightarrow e\nu W$.

The detector "simulation" is performed by smearing final state particles with gaussians whose widths have been determined by detailed studies of the SLD detector Monte Carlo. This four-vector analysis has been developed to maximize the mass-resolution of the detector, and hence uses the tracking chambers as much as possible. All charged track energies are derived from the track momentum. All neutrals that are not associated with a charged track receive their energies from the calorimeter, and thus the energy resolution on isolated neutrals is given by that of the calorimeter itself. The energies for neutrals that happen to overlap with charged track showers in the calorimeter are extracted by removing the appropriate energy of the charged track and assigning the remainder to the independent neutral. This maintains good resolution for hadronic neutrals in jets, but the resolution for electromagnetic showers in jets degrades substantially. A complete list of the resolutions used is given in Table 3. Note that the resolutions used here are not that different from those of existing detectors; state-of-the-art

Particle Type		Resolution
charged tracks		$\sigma(p)=.0015p$
isolated neutrals	EM:	$\sigma(E)=8\%/\sqrt{E} \oplus 1.5\%$
	HAD:	$\sigma(E)=55\%/\sqrt{E} \oplus 12\%$
neutrals in jets	EM:	$\sigma(E_{jet})= 5\times\sigma(E)$
	HAD:	$\sigma(E_{jet})=1.2\times\sigma(E)$

Table 3. Resolutions used in the smearing of final state particles for these analyses. See the description in the text for details.

calorimetery is not required for these analyes. All leptons are considered to be indentified with 100% accuracy, although in reality none of the analyses would be adversely effected by the lepton identification efficiencies obtained with existing detectors. In addition, all tracks with less than 150MeV/c p_T and all particles within 10° of the beamline are removed.

C. Measurement of $\Gamma(H \rightarrow WW^{(*)})$

We present two complementary analyses to measure the branching fraction of the Higgs into W-bosons: one using the hadronic decay modes of both Ws, the second requiring one of the Ws to decay leptonically, via $W \rightarrow l\nu$.

- *Hadronic Decay Modes (6-jet Analysis)*

This analysis requires the reconstruction of the 6-jet final state containing the four jets from the Higgs and the two from the Z, and thus could be applied equally well to study the branching fraction for $H \rightarrow ZZ^{(*)}$. Since measurement of the jet-pair masses is crucial, cuts on visible energy and total longitudinal and transverse momentum are placed on the events to limit the amount of missing energy taken away by neutrinos or radiation. (A detailed list of cuts follows this description.) A containment cut is also placed on the direction of the thrust axis. To select events with ZH as the final state, the event is broken up into 6 jets, and the masses of all possible pairings are computed. The pair whose mass is closest to the mass of the Z is designated the Z candidate, and the event is rejected if this mass is not within 10 GeV of m_Z. The other four jets are called the Higgs, and their mass is required to be within 10 GeV of the Higgs mass. To further reject background, the angle between the two jets from the Z is required to be less than 90°, and the angle between the two jets that comprise the real W from the higgs decay is required to be less than 120°. The analysis is summarized pictorially in Figure 9.

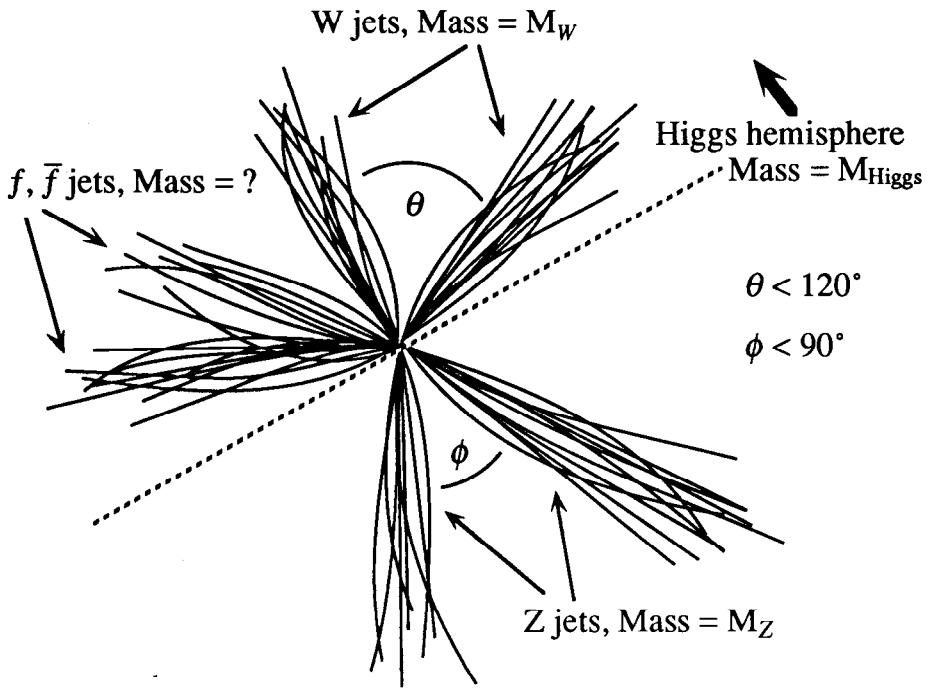

Figure 9. A pictorial summary of the 6-jet analysis.

Once the event has been selected for the ZH final state, several cuts are applied to select specifically for the 6-jet final state where the Higgs decays to 4 jets. The first of these, which generally removes events with a 4-jet final state, is to require that the y_{cut} for the 6-jet solution returned from the JADE cluster-finding algorithm [7] is greater than 8×10^{-4}. This cut is based on the knowledge that, due to the large masses of the Z and Higgs, jets tend to be well-separated in the final state. This is true even if the Higgs decays to a boson virtual-boson pair (a three-body decay), since the invariant mass spectrum of the virtual boson decay products is peaked towards the maximum value allowed kinematically [8]. If the Higgs decays to two fermions, the two jets are usually very distinct, and the entire event clearly has four jets. In order for this event to be constrained into a 6-jet solution two of the jets have to be split, leaving the largest allowed combination of invariant masses where 6 jets still exist as a relatively small fraction of the total visible energy, and hence a small value of y_{cut}. The distribution of y_{cut} values for the 6-jet solution in $H\rightarrow WW^{(*)}$ and $H\rightarrow b\bar{b}$ events is shown in Figure 10.

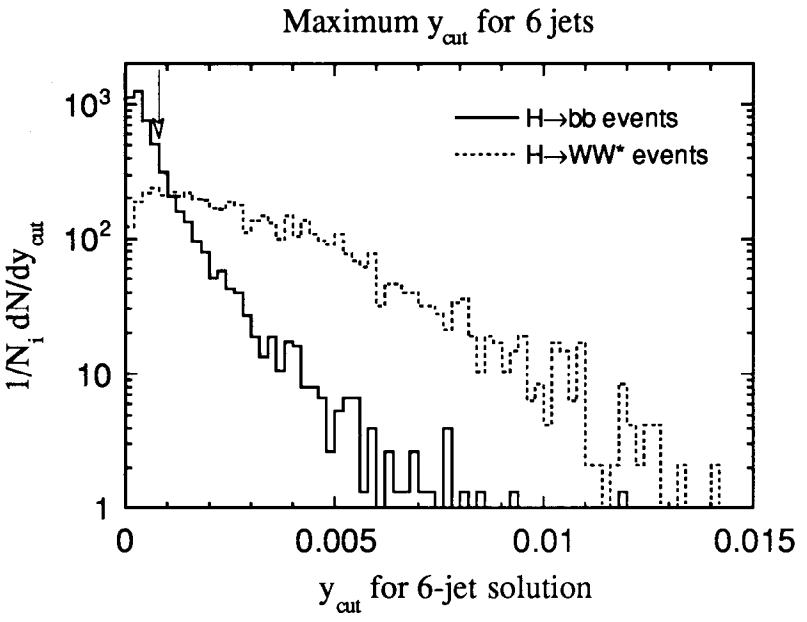

Figure 10. Distributions for the maximum allowable y_{cut} value such that the event contains 6 jets, shown for typical 4-jet events ($H \rightarrow b\bar{b}$) and typical 6-jet events ($H \rightarrow WW^{(*)}$). The arrow shows where the cut was placed. Note the log scale of the vertical axis.

In order to remove the background Higgs decay mode with the largest expected rate, an anti-B tag is applied, requiring that there be less than or equal to 3 tracks with significant large impact parameters per event. The complete list of cuts is as follows:

- $E_{vis} > .8\ E_{CM}$
- $\Sigma p_T < 20$ GeV, $\Sigma p_z < 30$ GeV
- $\left|\cos\theta_{Thrust}\right| < .7$
- 6 jets in the event
- y_{cut} for 6-jet solution $> 8\times10^{-4}$
- Angle between W jets $< 120°$
- Angle between Z jets $< 90°$
- $\left|\text{2-jet mass} - M_Z\right| < 10$ GeV
- $\left|\text{4-jet mass} - M_{Higgs}\right| < 10$ GeV
- Anti-B tag:

  <3 tracks with $b_{norm}>3$

- $|\text{2-jet mass} - M_W|$ < 10 GeV

The signal events then contain 4 jets coming from the Higgs, two of which combine to a mass close to m_W, with the other two resulting in an invariant mass lower than the kinematic limit of about 60 GeV for a Higgs mass of 140 GeV. Figure 11(a) shows the mass combinations for the pairings of the 4 jets (signal events only), where the one identified as the W is the pair with a mass closest to m_W. Figure 11(b) shows the results of the analysis, where the signature is that there is a real W reconstructed with a mass within 10 GeV of m_W, and that the smaller mass pair (the $f\bar{f}$ pair) have a mass less than 60 GeV. The events counted as lying within the signal region are those where the $f\bar{f}$ pair have a mass between 20 GeV and 60 GeV. Assuming Standard Model Higgs couplings, this analysis gives a signal of 17.7 events over a background of 39.4 events. (See Table 4.)

- *Leptonic Decay Modes (Missing Momentum Analysis)*

This analysis takes advantage of the large branching fraction for the W to decay to leptons, and thus has completely different systematics from the method described above. The strategy is to choose events with one high-momentum, isolated lepton, and then fit for the missing momentum carried off by the neutrino, as was sketched briefly with regard to Figure 7. The events are selected to contain 4 jets, with the pair whose mass is closest to m_Z being denoted the Z for analysis purposes. There are no cuts placed on total visible energy or missing momentum, but a cut is placed on $\cos\theta_{\text{Thrust}}$ to make sure the event is well contained in the detector. Cuts on the isolation of the lepton and the direction of the missing momentum remove background events from heavy quark decays and $e^+e^- \rightarrow ZZ$ events where one of the Zs decays into two leptons and one is lost. The cut on the angle between the two hadronic systems of the Z and the $W^{(*)}$ removes $e^+e^- \rightarrow W^+W^-$ events, since only one of the Ws can decay hadronically, placing the required 4 jets very close

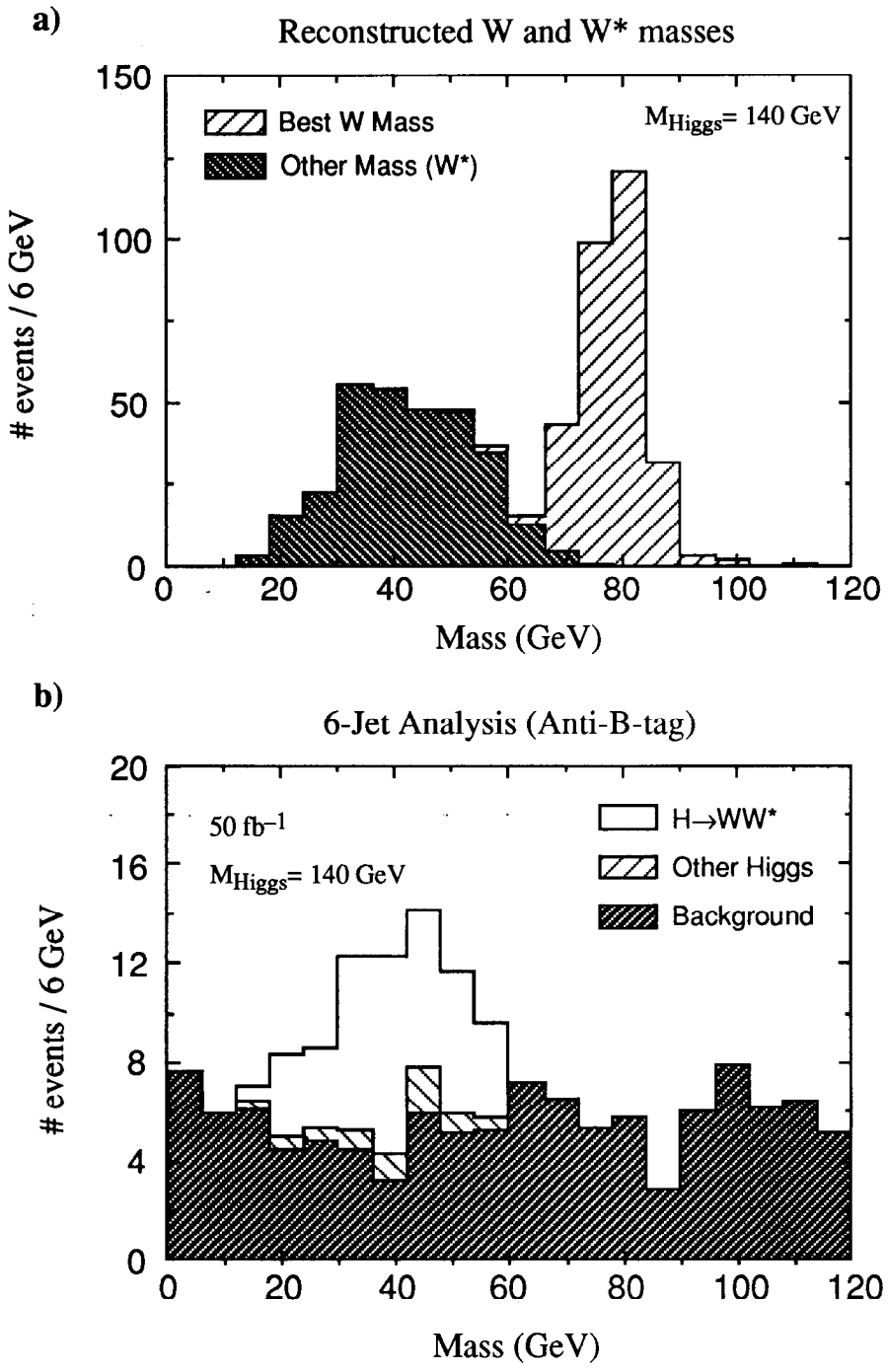

Figure 11. (a) The distribution of jet masses within the 4 jets from the Higgs decay. Note that the mass from the $f\bar{f}$ pair from the W^* follow the distribution expected from the kinematics of this decay. **(b)** Final results of the analysis, after all cuts. A signal of $H \rightarrow WW^*$ events represented by the reconstructed W^* can be seen clearly above 50 fb^{-1} of background. The number of signal events assumes the branching fractions for a Standard Model Higgs.

together in the final state. In addition, an anti-B tag is applied to remove any residual $t\bar{t}$ events. A complete list of cuts follows:

- $\left|\cos\theta_{\text{Thrust}}\right| < .7$
- Angle between W and Z jets > 90°
- $\left|\text{2-jet mass} - M_Z\right| \quad < 10$ GeV
- One and only one lepton of $p > 15$ GeV
- p_T of lepton with respect to the nearest jet > 5 GeV
- The missing momentum direction have $\left|\cos\theta_{\text{pmiss}}\right| < .983$
- Anti-B tag:

  <3 tracks with b_{norm}>3

Events which satisfy these cuts are then subject to a 0-C fit with the following constraints:

- $E_{\text{vis}} = 2\, E_{\text{beam}}$
- $\sum p_x = \sum p_y = 0$
- $\sum p_z + p_{\text{ISR}} = 0$
- $M_{\text{Higgs}} = \text{Mass}(\text{ lepton + neutrino + } W^{(*)} \text{ jets})$

For more accurate energies to input to the fit, the energy of the Z was rescaled so that $E_Z = \gamma_{\text{obs}}\, m_Z$, where γ_{obs} is calculated from the measured β_Z. The varibles of the fit are the three components of the neutrino momentum $p_{\nu x}$, $p_{\nu y}$, $p_{\nu z}$, the momentum of the initial-state radiation photon p_{ISR}, and the energy of the hadronic W or W^* system $E_{W^{(*)}}$. Figure 12 shows the resulting distribution of the invariant mass from the fitted neutrino momentum and that of the isolated lepton, where an additional requirement that the χ^2 of the 0-C fit be less than 20 has been imposed. Assuming Standard Model couplings for the Higgs, the number of $H \rightarrow WW^*$ events in the signal region around the peak at m_W is 24.3 over a background of 62.2 events. As one can see from the plot, the signal in this mode is marginal. This analysis in particular *would* benifit from improved calorimeter resolution, as the visible partons are reconstructed without benefit of beam-energy constraints.

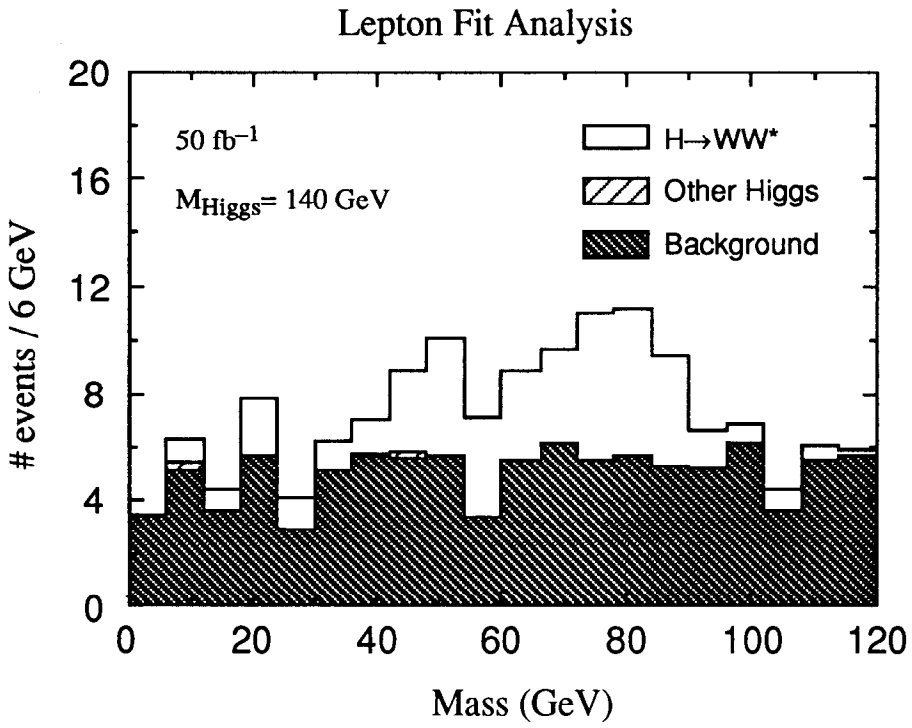

Figure 12. The resulting lepton-neutrino mass for $H \rightarrow WW^*$ events over 50 fb^{-1} of background events. Those taken as "signal" are those with the lepton-neutrino mass within 20 GeV of the W mass. The number of signal events is normalized assuming Standard Model branching fractions for the Higgs.

D. Measurement of $\Gamma(H \rightarrow b\bar{b})$ or $\Gamma(H \rightarrow c\bar{c} + gg)$

This analysis takes advantage of the 4-jet nature of these events to exclude the Higgs decays to vector bosons. Either a B-tag or anti-B-tag is then applied to select events with b or light quarks, respectively. The event selection cuts are in most cases identical to those for the 6-jet $H \rightarrow WW^*$ final state analysis presented above, with several exceptions. Here, 4 jets are required in the final state, and the jet energies are rescaled, keeping the jet angles fixed [9]. In addition, once the two events comprising the Z are identified, the maximum y_{cut} for the Higgs portion of the event to contain 3-jets is computed, and required to be small. This rejects the $H \rightarrow VV^*$ events,

which tend to have at least 3 jets coming from the decays of the vector bosons. The complete list of cuts is as follows:

- $E_{vis} > .8\ E_{CM}$
- $\sum p_T < 20$ GeV, $\sum p_z < 30$ GeV
- $\left|\cos\theta_{Thrust}\right| < .7$
- 4 jets in the event
- y_{cut} for 3-jet solution on Higgs $< 1.8\times10^{-2}$
- Angle between Higgs jets $< 120°$
- Angle between Z jets $< 90°$
- $\left|\text{2-jet mass} - M_Z\right| < 10$ GeV
- Anti-B tag:

  <3 tracks with $b_{norm}>3$

– OR:

- B-tag:

  ≥ 3 tracks with $b_{norm}>3$

The results of this analysis for $H\rightarrow b\bar{b}$ events are shown in Figure 13(a), which shows a signal of 116.8 events over a background of 109.2 events within 20 GeV of the Higgs mass. Figure 13(b) shows the acceptance of this analysis with the anti-B-tag applied for the different Standard Model decay modes of the Higgs. Note that the acceptance for the light quark and gluon modes is quite large compared to any other modes. This method will almost certainly be used to isolate a relatively pure sample of light quark events, and thus extract an exclusive measurement of the branching fraction for $H\rightarrow c\bar{c}$ events.

E. Measurement of $\Gamma(H\rightarrow\tau^+\tau^-)$

This analysis is similar to that presented by P. Janot in these proceedings [10]. Since the Higgs is so much more massive than the τ, the τs in the $H\rightarrow\tau^+\tau^-$ decay receive a tremendous boost. Thus, to

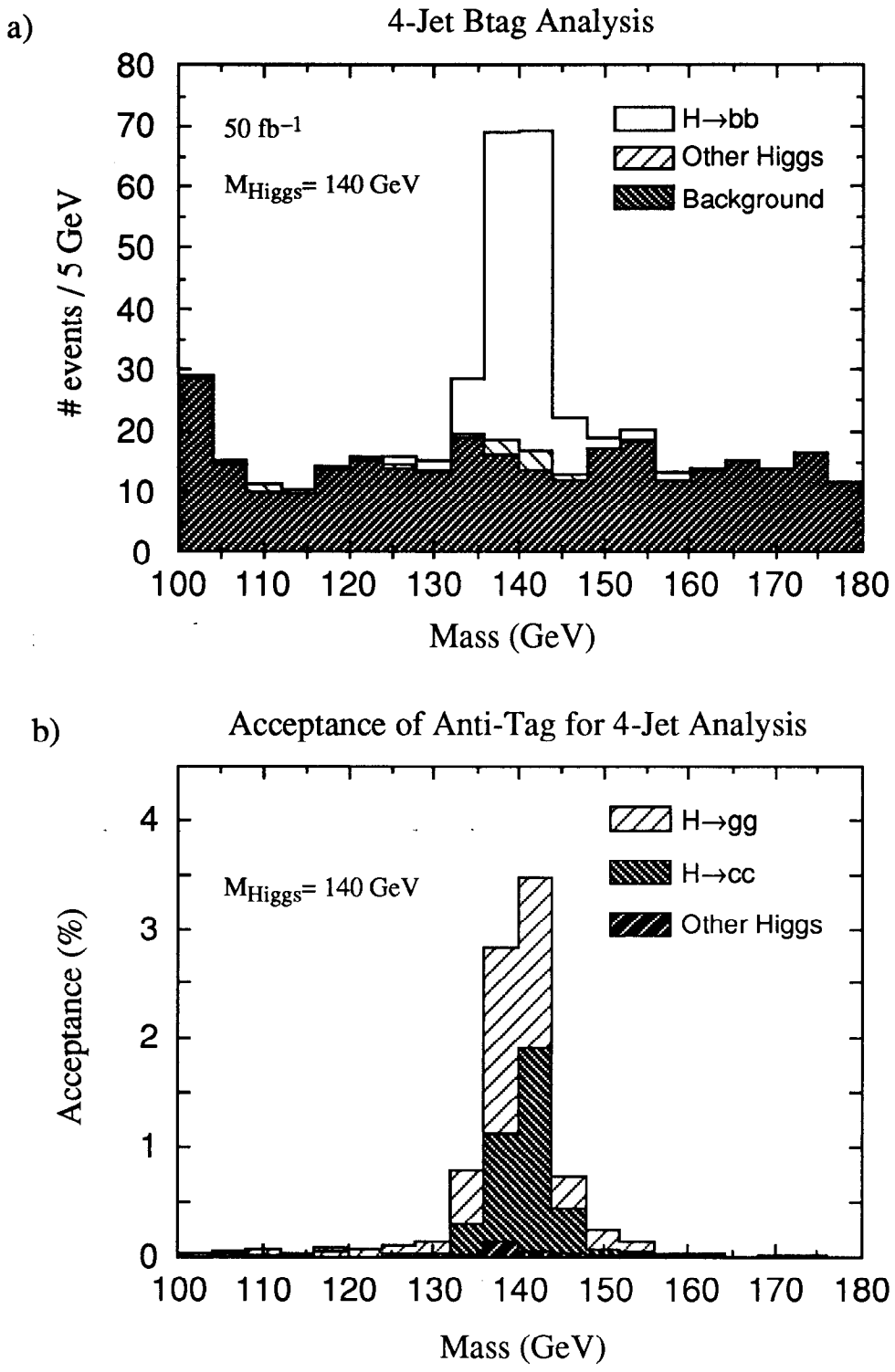

Figure 13. **(a)** Results of the 4-jet analysis with B-tagging applied to isolate events containing *b* quarks. An integrated luminosity of 50 fb^{-1} and Standard Model branching fractions for the Higgs are assumed. **(b)** Acceptance in percent of this analysis for events containing lighter quarks, where an anti-B-tag has been applied.

a good approximation, the decay products of the τ fall into a very narrow cone along the initial τ-direction. Since we know the center-of-mass energy and momentum, we can reconstruct the initial τ energies and the recoiling Z. At this stage, it is not neccessary to use our (assumed) knowledge of the Higgs mass except to provide initial values for the fit. We only consider here the 1-prong decay modes of the τ for simplicity.

The events are required to have some missing energy, be contained within the detector, and have a minimum number of charged particles to eliminate background from $e^+e^- \rightarrow ZZ$ events. Candidates for the two tau decay products are chosen by selecting the two most isolated particles in the event, where isolation ρ is defined below. These particles must be of high momentum, be less than 120° apart, and have opposite charges. In addition, when these particles plus any associated neutrals within a cone of 10° around the particle direction are subtracted from the event the remainder must have a mass within 10 GeV of the Z mass. The final kinematic requirement is that they lie within a plane containing the Higgs (Z) momentum. The detailed list of cuts is as follows:

- $E_{vis} < .8\ E_{CM}$
- >10 charged particles
- $\left|\cos\theta_{Thrust}\right| < .7$
- Find two most isolated particles, where isolation ρ is defined by

$$\rho_i = \min\sqrt{E_i\,(1-\cos\theta_{ij})}$$

- $\min(\rho_1,\rho_2) > 2.$, and $p_{1,2} > 5$GeV
- sum of charges=0
- opening angle < 120°
- subraction of isolated tracks + all neutrals within cones of 10° gives:
- $\left|\text{2-jet mass} - M_Z\right| \quad < 8$ GeV
- Acoplanarity of "taus" along Higgs axis < 11.5°

The energies of the taus and the recoiling Z are then extracted from a 0-C fit subject to energy and momentum constraints. Figure 14 shows the invariant mass of the two taus after their energies have been extracted from the fit. Note that this particular analysis results in extremely low background contamination to the $H \rightarrow \tau^+\tau^-$ sample. There are 17.4 signal events over a background of 3 events within 15 GeV of the Higgs mass.

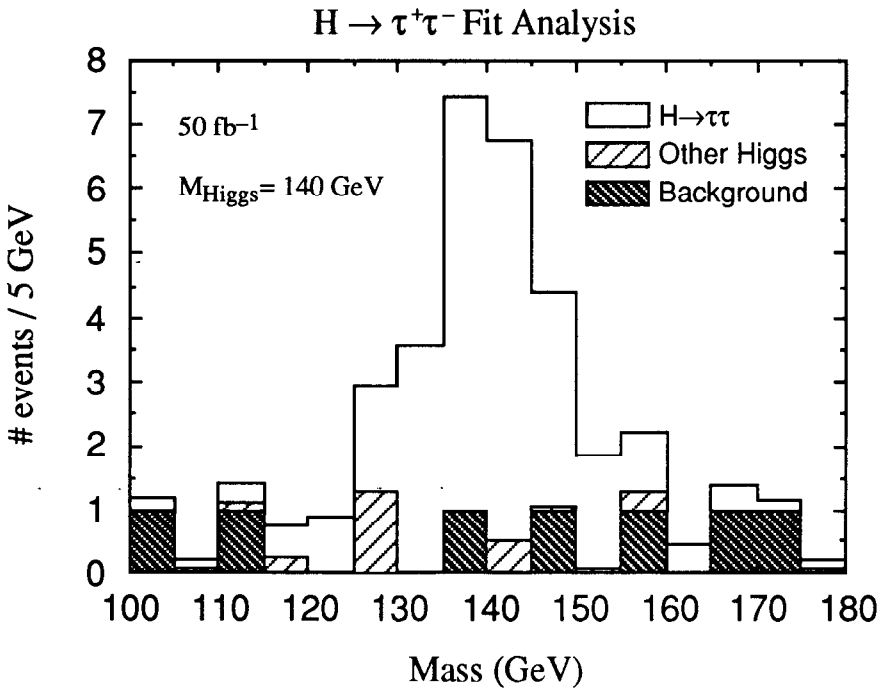

Figure 14. Mass distribution of the tau pairs reconstructed by a kinematic assuming a recoiling Z opposite two particles. See text for a more detailed description. The Standard Model branching fractions for the Higgs have been assumed to make this plot.

F. Measurement of the top-Higgs Yukawa coupling, g^2_{ttH}

Here we present two methods of determining the *ttH* Yukawa coupling, one for a heavy Higgs and one for a lighter Higgs.

• *For* $m_{Higgs} > 2\ m_{top}$

In the case of a heavy Higgs that can decay directly to top quarks, the coupling of the Higgs to the top can be measured directly by a determination of the branching fraction for $H \rightarrow t\bar{t}$ [11]. This is resonant production via the process shown in Figure 15.

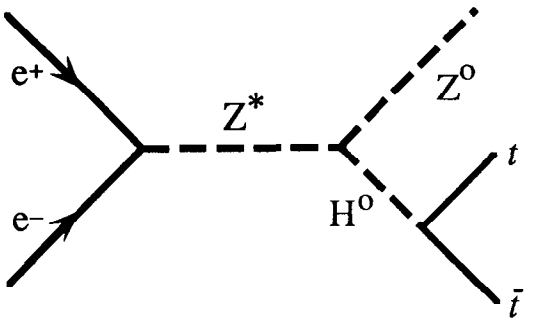

Figure 15. Resonant production of the $Zt\bar{t}$ final state when $m_{\text{Higgs}} > 2\ m_{\text{top}}$.

The signal for these events is an 8-jet final state: $WbWbf\bar{f}$. The energies of the jets are fitted with constraints to m_W, m_{top}, m_{Higgs}, and m_Z, and the $t\bar{t}$ mass is reconstructed.

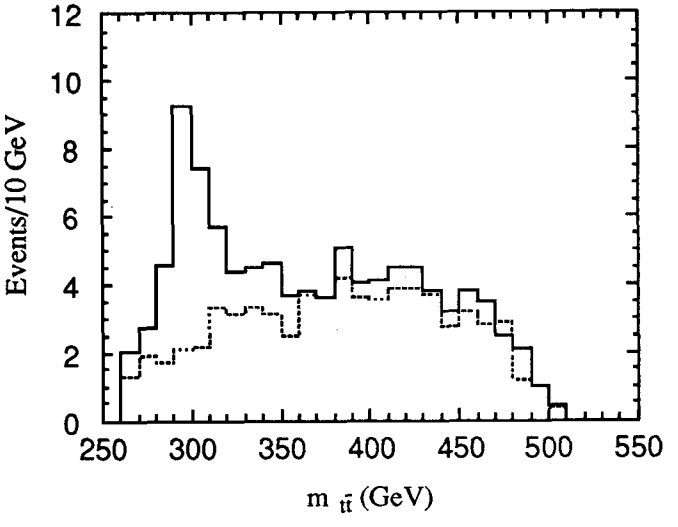

Figure 16. The resulting $t\bar{t}$ mass spectrum for m_{Higgs} = 300 GeV (solid line) and non-resonant production (dotted line) for a top mass of 130 GeV.

The only possible background is from non-resonant production of the $Zt\bar{t}$ final state through ordinary Z-γexchange. The results for this analysis based on 60 fb^{-1} at $\sqrt{s}$ = 600 GeV for a top mass of 130 GeV is shown in Figure 16. The resulting signal of 25 events over a background of 10 gives an error of 25% on g^2_{ttH}.

• *For* $m_{Higgs} < m_{top}$

If the Higgs is light enough compared to the top mass, the Higgs bremsstrahlung process shown in Figure 17. will occur at measureable rates, summarized by the plots in Figure 18. [12]

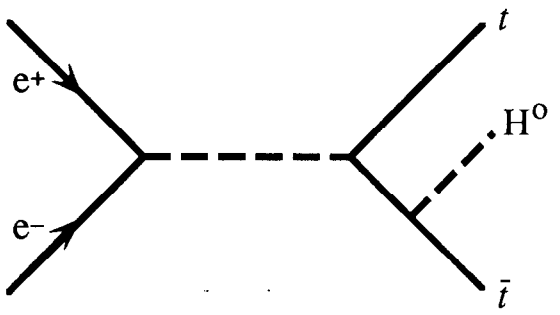

Figure 17. The $t\bar{t}H$ bremsstrahlung process for $m_{\text{Higgs}} < m_{\text{top}}$.

The signature for these events is quite spectacular: 8 jets, with *WbWbbb*. There should be absolutely no background whatsoever, as there is no other case when one might find 4 jets containing *b* quarks in an event. Including an estimate of tagging efficiency for these events, it is estimated [Burke] that for $\sqrt{s}$ = 1 TeV and 50 fb^{-1} of integrated luminosity one could detect 100-200 of these events for reasonable top and Higgs masses, which would yield a 10% measurement of g^2_{ttH}.

IV. Summary and Conclusions

Table 4 contains a numerical compilation of the results for the measurements of the Higgs branching fractions presented in the

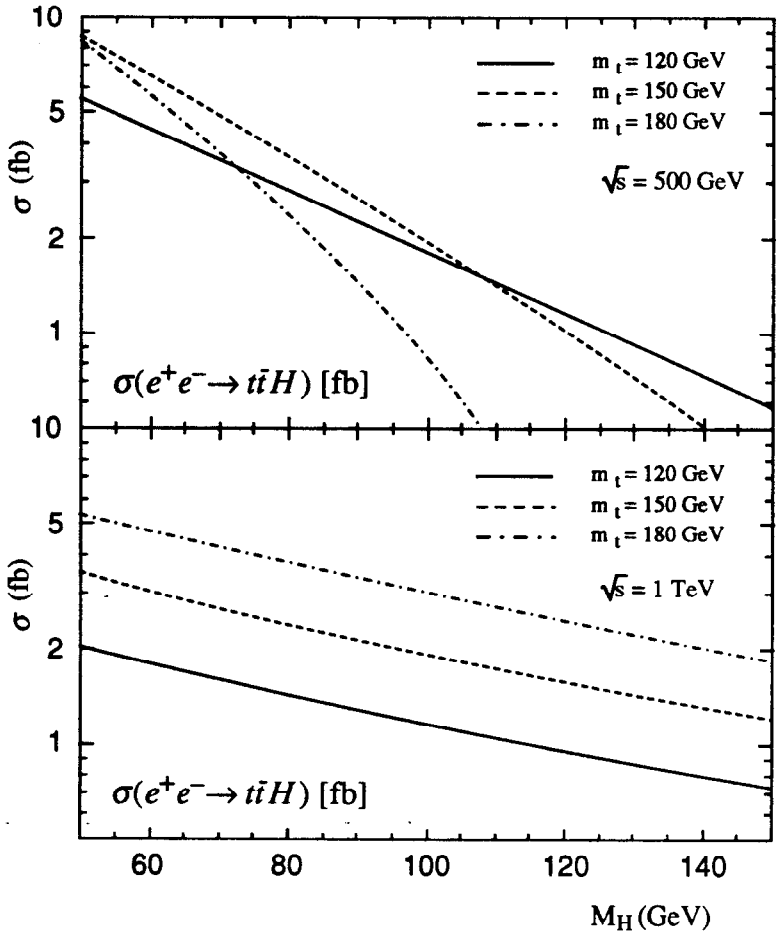

Figure 18. Production cross sections for the process $e^+e^- \rightarrow t\bar{t}H$ for a variety of Higgs and top masses. The top plot is for $\sqrt{s}$ = 500 GeV, the bottom for $\sqrt{s}$ = 1 TeV.

above section. For each analysis the "signal" region used is the one defined in the above descriptions. To calculate the signal-to-noise ratios for each analysis, the Standard Model branching fractions were assumed for a Higgs with mass 140 GeV. The assumed integrated luminosity is 50 fb^{-1}. Figure 19(a) shows the expected errors for the measurements of the branching fractions for the Standard Model Higgs boson, where the numerical results are summarized in Table 5. Figure 19(b) shows the expected errors on the Standard Model branching fractions compared to the branching fractions predicted for a 140 GeV *CP*-even MSSM Higgs.

As can be seen from these calculations, many of the Standard Model decay modes of the Higgs are accessible to experimental consideration. It is possible to obtain detailed measurements of the Higgs-fermion and Higgs-boson couplings with approximately one year of running at peak luminosity, even with these relatively simple analyses. In fact, most of the measurements have on the order of 20% errors. The one exception is the measurement of the branching fraction for $H \rightarrow c\bar{c}$ + $H \rightarrow gg$, which can only be used to give an upper limit at this time. More complicated analyses will be neccessary to extract independent measurements of these two branching fractions, and these are being pursued at this time. However, note the vast difference in the expected branching fraction for $H \rightarrow WW^*$ between the Standard Model and MSSM case, as shown in Figure 19(b). Since this decay is dominant for a Standard Model Higgs of mass greater than 140 GeV, yet still has a branching fraction of 10% down to a mass of 120 GeV (see Figure 5(a)), a measurement of this branching fraction should prove to be a powerful discriminatory tool to understand the nature of a discovered Higgs particle.

	Tag Efficiencies:				
Decay Mode	4-jet B-tag	4-jet Anti-tag	6-jets	Lepton Fit	Tau fit
$H \to b\bar{b}$	5.67%	0.24%	<0.1%	<0.1%	<.01%
$H \to WW^*$	0.11%	0.23%	1.39%	1.45%	0.03%
$H \to ZZ^*$	0.07%	0.36%	0.76%	<0.1%	0.04%
$H \to c\bar{c} + H \to gg$	3.72%	5.80%	0.75%	<0.1%	<0.1%
$H \to \tau^+\tau^-$	<0.1%	<0.1%	<0.1%	0.42%	11.5%
Background ($50fb^{-1}$)	109.2 events	196.9 events	39.4 events	62.2 events	3 events
Signal-to-Noise*	1.07 : 1	0.06 : 1	0.45 : 1	0.39 : 1	5.8 : 1

*Standard Model Branching fractions assumed ($50fb^{-1}$), M_{Higgs} = 140 GeV

Table 4. Results from the analyses to measure the branching fractions of the Higgs boson.

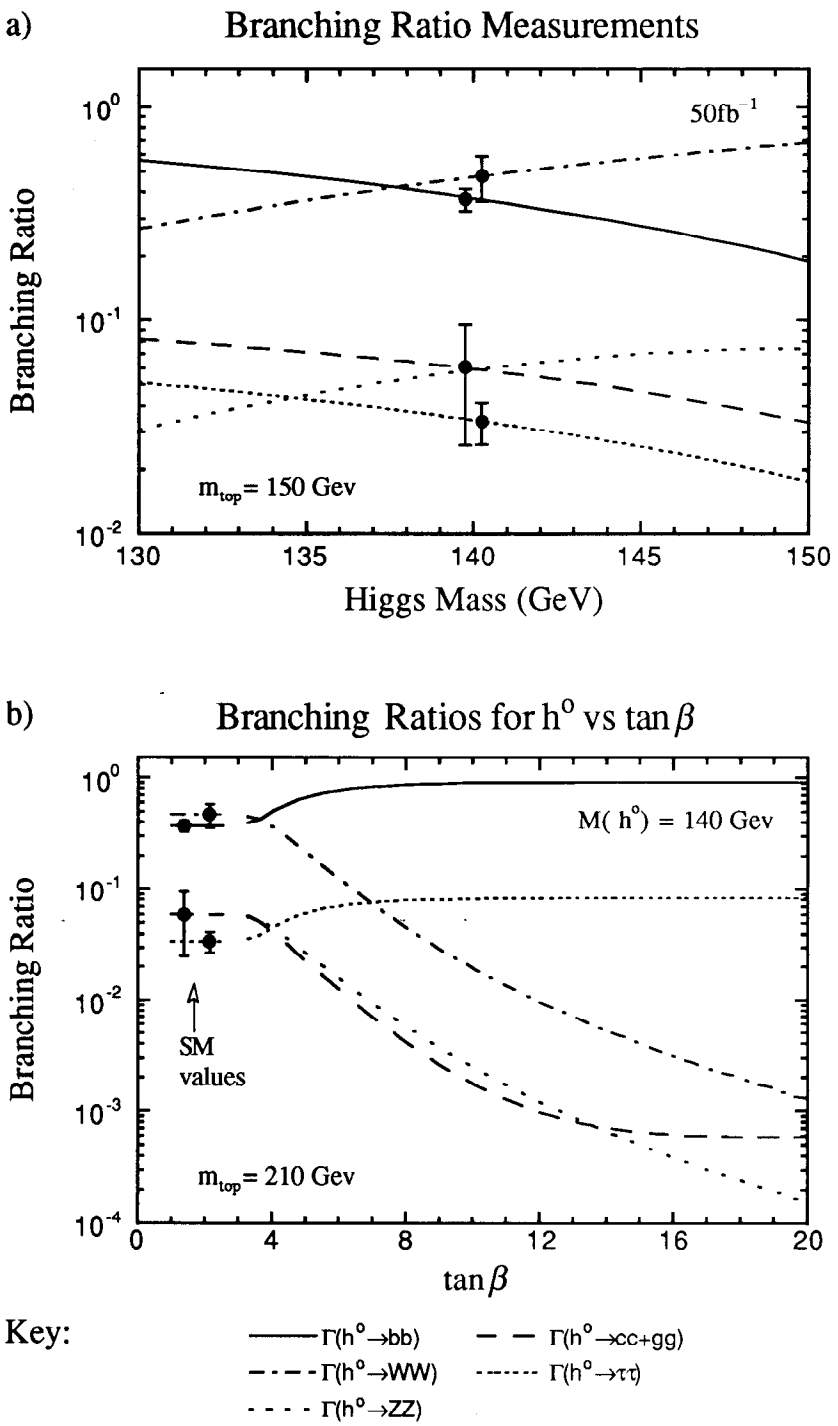

Figure 19. (a) Expected errors on the measurement of the Standard Model branching fractions for a Higgs mass of 140 GeV. The points have been displaced slightly to allow the error bars to be seen. This plot assumes an integrated luminosity of 50 fb^{-1} and Standard Model couplings for the Higgs. (b) Expected errors on the Standard Model branching fractions with the predicted branching fractions for a 140 GeV *CP*-even MSSM Higgs. Note the somewhat extreme top quark mass needed for the scalar mass to be this large.

Branching Fraction	Expected error
$\frac{\sigma(\sigma_{tot} \times \Gamma(H \to b\bar{b}))}{\sigma_{tot} \times \Gamma(H \to b\bar{b})}$	= ± 12%
$\frac{\sigma(\sigma_{tot} \times \Gamma(H \to WW^*))}{\sigma_{tot} \times \Gamma(H \to WW^*)}$	= ± 24%
$\frac{\sigma(\sigma_{tot} \times \Gamma(H \to c\bar{c}+gg))}{\sigma_{tot} \times \Gamma(H \to c\bar{c}+gg)}$	= ± 116%
$\frac{\sigma(\sigma_{tot} \times \Gamma(H \to \tau^+\tau^-))}{\sigma_{tot} \times \Gamma(H \to \tau^+\tau^-)}$	= ± 22%
For *ttH* Bremsstrahlung (lighter Higgs):	
$\frac{\sigma(g_{ttH}^2)}{g_{ttH}^2}$	= ± 10%
For *ttH* resonant production (Heavy Higgs):	
$\frac{\sigma(g_{ttH}^2)}{g_{ttH}^2}$	= ± 25%

Table 5. The numerical values of the errors shown on the plots in **Figure 19**. The errors for those branching fractions excluding the top quark are calculated assuming Standard Model coupling for the Higgs and 50 fb^{-1} of integrated luminosity at $\sqrt{s}$=400 GeV. Note that one actually measures the total cross section multiplied by the branching fraction, as there could be other, invisible decay modes. The error on g_{ttH}^2 for the light Higgs case assumes 50 fb^{-1} at $\sqrt{s}$=1 TeV. The error on g_{ttH}^2 for the heavy Higgs case assumes 60 fb^{-1} at $\sqrt{s}$=600 GeV.

References:

[1] S.L. Glashow, Nucl. Phys. **B22** (1961) 579;
S. Weinberg, Phys. Rev. Lett. **19** (1967) 1264;
A. Salam, Proc. 8th Nobel Symposium, Stockholm 1968, ed. N. Svarthholm (Almquist and Wiksells, Stockholm, 1968) p.367

[2] E. Witten, Nucl. Phys. **B188** (1981) 513;
S. Dimopoulos and H. Georgi, Nucl. Phys. **B193** (1981) 150;
N. Sakai, Z. Phys. **C11** (1981) 153

[3] For a review of the design paramters for linear colliders (present and future) see R.B. Palmer, Annu. Rev. Nucl. Part. Sci. **40** (1990) 529 and references within.

[4] T.L. Barklow, P. Chen, W.L. Kozanecki, *"Beamstrahlung Spectra in Next Generation Linear Colliders"*, in e^+e^- *Collisions at 500 GeV: The Physics Potential*, DESY 92-123, ed. P. Zerwas, p. 845; SLAC-PUB-7063

[5] This Figure and Figure 19 were produced using the results of calculations by H. Haber and R. Hempfling (H. Haber, private communication).

[6] D. Su, *"A Preliminary Measurement of R_b at SLD"*, presented at D.P.F., Dallas, 1992

[7] JADE Collab., W. Bartel *et al.*, Z. Phys. **C33** (1986) 23

[8] W.Y. Keung and W.J. Marciano, Phys. Rev. **D30** (1984) 248

[9] Sau Lan Wu, Z. Phys. **C9** (1981) 329;
T.L. Barklow, *"A Search for the Production of Charged Higgs and Technipions with Large Hadronic Branching Ratios in e^+e^- Annihilation at 34.5 GeV Center-of-Mass Energy"*, Wisconsin Thesis, 1983.

[10] P. Janot, *"Light Higgs Spectrum from e^+e^- Annihilation"*, proceedings of *"Electroweak Symmetry Breaking at Colliding-Beam Facilities"*, Santa Cruz, CA, December 11-12, 1992

[11] T. Tauchi, K. Fujii, A. Miyamoto, Proc. Snowmass '90 Summer Study on High Energy Physics, ed. E.L. Berger, p. 456

[12] A. Djouadi, J. Kalinowski, and P. Zerwas, Z. Phys. **C54** (1992) 255